J. Biochem. 130, 553–559 (2001)

Antibody–Antigen Interactions Measured by Surface Plasmon Resonance: Global Fitting of Numerical Integration Algorithms

Jie Luo,* Junmei Zhou,*,[1] Wei Zou,† and Ping Shen†

*National Laboratory of Biomacromolecules, Institute of Biophysics, Academia Sinica, Beijing 100101, China; and †Beijing Amersham Pharmacia Biotechnology Centre, Beijing 100101, China

Received June 8, 2001; accepted August 6, 2001

The interactions between adenylate kinase (AK) and a monoclonal antibody against AK (McAb3D3) were examined by means of optical biosensor technology, and the sensograms were fitted to four models using numerical integration algorithms. The interaction of a solution of McAb3D3 with immobilized AK follows a double exponential function and the data fitted well to an inhomogeneous ligand model. The interaction of a solution AK with immobilized McAb3D3 follows a single exponential function and the data fitted well to a pseudo-first order reaction model. The true association constants of AK binding to McAb3D3 in solution were obtained from competition BIAcore measurements. The difference in results obtained with solid-phase BIAcore and competition BIAcore may be due to rebinding of the dissociated analyte to the immobilized surface. The results obtained with BIAcore are compared to those obtained by ELISA methods. We suggest that the best method for analysis of BIAcore data is direct, global fitting of sensorgrams to numerical integration algorithms corresponding to the different possible models for binding.

Key words: adenylate kinase, inhomogeneity, monoclonal antibody, optical biosensor, sensorgram.

Adenylate kinase is an important enzyme in energy metabolism which catalyzes the reversible phosphoryl transfer between ATP and AMP. The rabbit muscle cytosolic enzyme comprises 194 amino acids in a single peptide chain (*1*). It has become a model protein for the study of the mechanisms and characteristics of kinase catalysis and folding (*2–9*). To study the conformational changes involved in the folding process, monoclonal antibodies have been raised against this protein and some aspects of their association with AK have been investigated (*10*). McAb3D3 is an IgG_1 subclass monoclonal antibody with a total molecular weight of 151.2 kDa, a heavy chain molecular weight of 51.6 kDa and a light chain molecular weight of 24.0 kDa (*11*). In order to characterize these protein–protein interactions quantitatively, the interaction between AK and McAb3D3 was studied by means of optical biosensor technology.

Surface plasmon resonance (SPR) detectors, such as the BIAcore (Amersham-Pharmacia), allow the direct visualization of these macromolecular interactions in real-time, and thus provide kinetic information in addition to the equilibrium binding constants. A further advantage of the method is the lack of requirement for labeling either the antigen or antibody, a process that may alter the affinity of the labeled species. The BIAcore method usually assumes that the interaction between soluble analytes and immobilized ligands can be described by pseudo-first-order kinetics in situations where constancy of the analyte concentration is maintained as the result of continual replenishment through the flow of the analyte solution across the sensor surface. However, quantitative kinetic analysis is often problematic and in most studies the data do not follow the expected ideal binding progress curve for a pseudo-first-order reaction (*12*). These deviations may be attributed to limitation of the mass transport from the bulk solution to the sensor surface or inhomogeneity of the binding sites (*13*). Inhomogeneous binding sites could be present intrinsically or produced extrinsically during immobilization. Since the chemical immobilization process may result in ligand binding with different affinities, a good test of this is whether or not the rate and equilibrium constants obtained by the solid phase BIAcore method correctly describe the interaction between an antibody and an antigen in solution.

In this study, we investigate the antigen-antibody interaction using the solid phase BIAcore method under conditions where AK and McAb3D3 are alternately used as the surface-coupled ligand. Systematic analysis of the BIAcore binding data by means of global fitting of numerical integration algorithms to the four possible models was first performed, and the rate and equilibrium binding constants were taken from the model which best fitted the data. The competition BIAcore experiments were performed under conditions where AK was used as the surface-coupled ligand to determine the rate and equilibrium binding constants in solution. The results obtained by these methods are compared to those obtained by ELISA methods.

[1] To whom correspondence should be addressed. Tel: +86-10-64889859, Fax: +86-10-64872026, E-mail: zhoujm@sun5.ibp.ac.cn

Abbreviations: AK, adenylate kinase [EC 2.7.4.3]; AMP, adenosine 5′-monophosphate; ATP, adenosine 5′-triphosphate; EDC, *N*-ethyl-*N*′-(3-diethylaminopropyl)-carbodiimide; ELISA, enzyme-linked immunosorbent assay; IgG, immunoglobulin G; NHS, *N*-hydroxysuccinimide; P20, 2-(2-pyridinyldithio)ethaneamine hydrochloride; RU, response unit; SPR, surface plasmon resonance.

MATERIALS AND METHODS

Instrumentation and Reagents—The BIAcore 1000 system, BIAevalution 3.0 software and reagents, including CM5 sensor chips, surfactant P20, and HBS buffer (10 mM Hepes with 0.15 M NaCl, 3.4 mM EDTA, and 0.05% surfactant P20, pH 7.4), and the amine coupling kit containing *N*-hydroxysuccinimide (NHS), *N*-ethyl-*N'*-(3-diethylaminopropyl)-carbodimide (EDC), and ethanolamine hydrochloride were provided by the Beijing Amersham-Pharmacia Biotechnology Centre.

Antigen and Antibody—Adenylate kinase was prepared from rabbit muscle and purified by the method described previously (*7*). The concentration of the purified AK was determined from the absorbance at 280 nm ($\varepsilon_{1\ mg/ml}$ = 0.52; MW 21,400 Da). The monoclonal antibody, McAb3D3, which was of the IgG subclass and raised against rabbit muscle adenylate kinase, was prepared as described previously (*11*). The concentration of McAb3D3 was determined from the absorbance at 280 nm ($\varepsilon_{1\ mg/ml}$ = 1.4; MW 151,200 Da). Other reagents were local products of analytical grade.

Immobilization of Ligands on the Sensor Surfaces—Immobilization of AK or McAb3D3 was performed as follows: (i) Equal volumes of NHS (50 μl, 0.06 M in water) and EDC (50 μl, 0.2 M in water) were first mixed, and then 70 μl of the resulting solution was pumped across the chip to activate the carboxymethylated dextran surface. (ii) 70 μl of ligand (75 μg/ml AK in 10 mM glycine, pH 6.0, or 134 μg/ml McAb3D3 in 10 mM glycine, pH 3.4) was then injected across the activated surface. (iii) Residual NHS-esters on the sensor chip surface were then inactivated with ethanolamine (50 μl, 1 M in water, pH 8.5). The immobilization was performed with a continuous flow of HBS at 10 μl/min.

Two surfaces were used in this experiment. For the first, AK was coupled to the dextran matrix via standard amine coupling chemistry using the amine coupling kit. The surface densities of AK obtained were 39 fmol/mm². For the second surface, McAb3D3 was coupled to the dextran matrix using standard amine-coupling chemistry. The surface densities of McAb3D3 obtained were 12 fmol/mm².

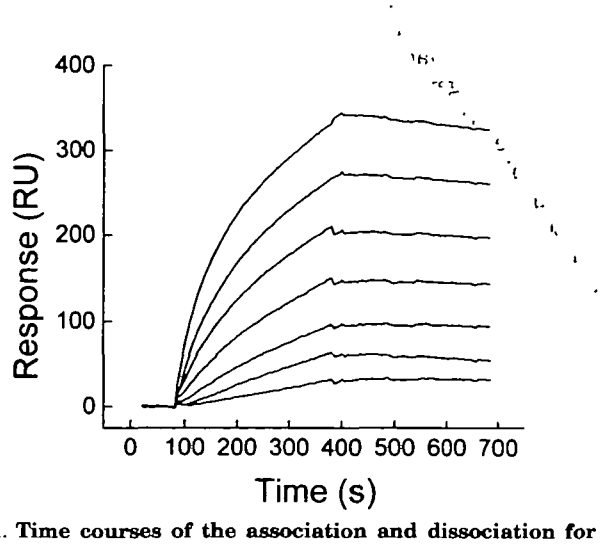

Fig. 1. **Time courses of the association and dissociation for McAb3D3 binding to immobilized AK.** AK was coupled at pH 6.0 and the surface density was 39 fmol/mm². From the bottom upwards, the McAb3D3 concentrations were 4.62×10^{-7}, 9.23×10^{-7}, 1.85×10^{-6}, 3.69×10^{-6}, 7.39×10^{-6}, 1.48×10^{-5}, and 2.95×10^{-5} M, respectively.

Binding Assays and Data Analysis—When the immobilized AK surface was used, 200 μl of McAb3D3 at various concentrations in HBS was injected at the flow rate of 40 μl/min. When the immobilized McAb3D3 surface was used, 40 μl of AK at various concentrations in HBS was injected at the flow rate of 20 μl/min. The dissociation process was initiated by injecting HBS only at the same flow rate as for sample injection for a further 300 s. The surface was regenerated by injecting 60 μl of 10 mM glycine (pH 2.0) between analyte injections. Sensors with immobilized AK and McAb3D3 appear to be able to withstand more than 100 regeneration cycles with no apparent loss of binding activity. Competition studies involving co-incubation of McAb3D3 with AK at a series of concentrations for 2 h at 37°C prior to injection were carried out. The experiments were performed at 19°C. Data were analyzed directly using numerical integration algorithms and the BIAevaluation 3.0 software (*14*).

RESULTS

Binding of McAb3D3 to Immobilized AK—Rabbit muscle AK was immobilized directly onto the sensor surface through covalent coupling of primary amine groups of AK to carboxyl groups on the dextran matrix, surface densities of 39 fmol/mm² being obtained. To determine the binding rate constants, seven different concentrations of McAb3D3, between 4.62×10^{-7} and 2.95×10^{-6} M, were used. The time courses of the binding and dissociation phases are shown in Fig. 1. The association between McAb3D3 and the immobilized AK was observed by following the increase in the

TABLE I. **Differential rate equations of various reaction models.**

Pseudo-first-order reaction model
$d[B]/dt = -(k_a \cdot [A] \cdot [B] - k_d \cdot [AB])$
$d[AB]/dt = (k_a \cdot [A] \cdot [B] - k_d \cdot [AB])$
$R = [AB] + RI$
Mass transport limitation model
$d[A_{sur}]/dt = k_t \cdot ([A_{bulk}] - [A_{sur}]) - (k_a \cdot [A_{sur}] \cdot [B] - k_d \cdot [AB])$
$d[B]/dt = -(k_a \cdot [A_{sur}] \cdot [B] - k_d \cdot [AB])$
$d[AB]/dt = (k_a \cdot [A_{sur}] \cdot [B] - k_d \cdot [AB])$
$R = [AB] + RI$
Inhomogeneous ligand model
$d[B]/dt = -(k_{a1} \cdot [A] \cdot [B] - k_{d1} \cdot [AB])$
$d[B']/dt = -(k_{a2} \cdot [A] \cdot [B'] - k_{d2} \cdot [AB'])$
$d[AB]/dt = (k_{a1} \cdot [A] \cdot [B] - k_{d1} \cdot [AB])$
$d[AB']/dt = (k_{a2} \cdot [A] \cdot [B'] - k_{d2} \cdot [AB'])$
$R = [AB] + [AB'] + RI$
Inhomogeneous analyte model
$d[B]/dt = -(k_{a1} \cdot [A] \cdot MW \cdot [B] - k_{d1} \cdot [AB])/MW - (2 \cdot k_{a2} \cdot [A_2] \cdot MW \cdot [B] - k_{d2} \cdot [A_2B])/(2 \cdot MW)$
$d[AB]/dt = (k_{a1} \cdot [A] \cdot MW \cdot [B] - k_{d1} \cdot [AB])$
$d[A_2B]/dt = (2 \cdot k_{a2} \cdot [A_2] \cdot MW \cdot [B] - k_{d2} \cdot [A_2B])$
$R = [AB] + [A_2B] + RI$

In these equations, *A* and *B* represent the analyte and surface-coupled ligand, respectively. *R* represents the instrument response and *RI* represents the response from the bulk refractive index effect. MW represents the molecular weight of the analyte (McAb3D3), which is 151.2 kDa. *AB*, *AB'*, and A_2B, which denote the molecular complexes formed during the reaction, are expressed in response terms. Thus, differential rate equations directly describe the binding curves obtained with the BIAcore sensor.

response values. The higher the McAb3D3 concentration, the larger the response values. When the sample injection ended at 380 s, the dissociation of the complexes present on the sensor surface was followed by a decrease in the response values. The resulting sensorgrams were fitted by global fitting to the four models: pseudo-first-order reaction, mass transport limitation, inhomogeneous ligands and inhomogeneous analytes, as described in Table I. Fitting of the data to the pseudo-first-order reaction mechanism and the mass transport limitation model gave similarly high χ^2 values (148 and 154, respectively; lines 1 and 2 of Table II). This indicates that neither of these models describes the binding of McAb3D3 to immobilized AK. The χ^2 value for fitting to the inhomogeneous analyte model is significantly lower (χ^2 = 24.1, line 4 of Table II). However, the best fit of the data is clearly with the inhomogeneous ligand model (χ^2 = 2.93, line 3 of Table II). The two distinct binding phases could be the result of two classes of immobilized AK on the chip surface with different binding affinities for McAb3D3. For the major class of immobilized AK, the magnitude of the equilibrium response (R_{max1}) is >75% of the total equilibrium response. The binding of the minor class of immobilized AK to McAb3D3 is apparently stronger than that of the major component.

Binding of AK to Immobilized McAb3D3—To determine whether the inhomogeneity of immobilized AK is present intrinsically or produced extrinsically during immobilization, the kinetics of binding of AK to immobilized McAb3D3 were examined. Six different concentrations of AK, between 2.12×10^{-6} and 6.78×10^{-5} M, were used to determine the rate constants. The time courses of the binding and dissociation phases are shown in Fig. 2. As the AK concentration increases, the response value increases. Because the molecular weight of AK is less than one-seventh of that of McAb3D3, the response values in Fig. 2 are lower than those in Fig. 1. When the sample injection ended at 200 s, the dissociation of the complexes present on the sensor surface was followed. The resulting sensorgrams were fitted by global fitting to the four models mentioned above. In this case the data fitted well to the simplest model, which is the pseudo-first-order reaction model (χ^2 = 2.74, Table III). This indicates that under experimental conditions with McAb3D3 as the surface-coupled ligand, both ligands and analytes were homogeneous. This suggests that the inhomogeneity of immobilized AK may be a result of immobilization.

Comparing the results obtained in these two experiments, we can clearly see that the equilibrium constant (K_a = 6.82×10^5 M^{-1}) of AK binding to immobilized McAb3D3 is similar to that for the major class of McAb3D3 binding to immobilized AK (line 3 of Table II). This indicates that most of the immobilized AK shows the same binding affinity to McAb3D3 as when it is in solution, and that only a small population of immobilized AK has an altered affinity.

Binding of Free Antibodies Equilibrated in an AK-McAb3D3 Mixture with Immobilized AK—To determine the affinity constant of AK binding to McAb3D3 in solution, the AK at various concentrations was first incubated in solution with McAb3D3 at a constant concentration until equilibrium was reached. After pre-incubation, the equilibrium mixture was injected onto the immobilized AK surface and the binding of free antibodies in this mixture to immobilized AK was analyzed. Since the BIAcore instrument uses a flow cell (60 nl volume), and the time of contact between

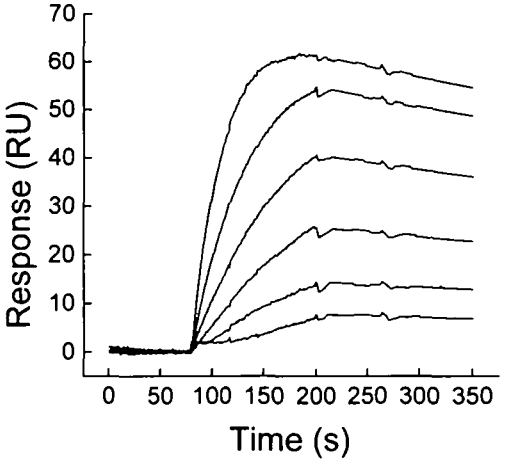

Fig. 2. **Time courses of the association and dissociation for AK binding to immobilized McAb3D3.** McAb3D3 was coupled at pH 3.4 and the surface density was 12 fmol/mm². From the bottom upwards, the AK concentrations were 2.12×10^{-6}, 4.23×10^{-6}, 8.47×10^{-6}, 1.69×10^{-5}, 3.39×10^{-5} and 6.78×10^{-5} M, respectively.

TABLE II. **The rate constants and equilibrium constant of McAb3D3 binding to immobilized AK.**

	R_{max1} (RU)	k_{a1} (M^{-1} s^{-1})	k_{d1} (s^{-1})	K_{a1} (M^{-1})	R_{max2} (RU)	k_{a2} (M^{-1} s^{-1})	k_{d2} (s^{-1})	K_{a2} (M^{-1})	k_t (s^{-1})	K (M^{-1})	χ^2
A	334	4.89×10^2	1.31×10^{-4}	3.72×10^6	—	—	—	—	—	—	148
B	332	5.08×10^2	1.47×10^{-4}	3.46×10^6	—	—	—	—	6.29×10^2	—	154
C	303	2.21×10^2	3.06×10^{-4}	7.21×10^5	95.4	2.06×10^3	$<10^{-6}$	$>10^{11}$	—	—	2.93
D	263	1.47×10^3	1.16×10^{-4}	1.26×10^7	—	2.62×10^2	$<10^{-6}$	$>10^{10}$	—	6.89×10^5	24.1

Curve fitting was performed according to various models: pseudo-first-order reaction (A), mass transport limitation (B), inhomogeneous ligand (C), and inhomogeneous analyte (D). Data were taken from Fig. 1.

TABLE III. **The rate constants and equilibrium constant of AK binding to immobilized McAb3D3.**

	R_{max1} (RU)	k_{a1} (M^{-1} s^{-1})	k_{d1} (s^{-1})	K_{a1} (M^{-1})	R_{max2} (RU)	k_{a2} (M^{-1} s^{-1})	k_{d2} (s^{-1})	K_{a2} (M^{-1})	k_t (s^{-1})	K (M^{-1})	χ^2
A	63.8	5.36×10^2	7.86×10^{-4}	6.82×10^5	—	—	—	—	—	—	2.74
B	63.6	5.63×10^2	8.04×10^{-4}	7.00×10^5	—	—	—	—	4.96×10^5	—	2.73
C	63.2	5.06×10^2	8.22×10^{-4}	6.15×10^5	1.37	1.99×10^4	1.07×10^{-6}	1.87×10^{10}	—	—	2.55
D	63.8	5.37×10^2	7.85×10^{-4}	6.84×10^5	—	6.45×10^{-3}	1.92×10^{-5}	3.36×10^2	—	66.1	2.72

Curve fitting was performed according to various models: pseudo-first-order reaction (A), mass transport limitation (B), inhomogeneous ligand (C), and inhomogeneous analyte (D). Data were taken from Fig. 2.

the complex and the chip surface is less than 0.09 s at the flow rate of 40 μl/min, negligible dissociation of the complex occurs during the contact time. Therefore, the equilibrium is not displaced when the antibody is captured from solution on the surface. Thus, the processes of binding of free antibodies to immobilized AK will follow the inhomogeneous ligands mechanism, as shown in Table II. For an antibody in the equilibrium mixture with two binding sites, immobilized AK can capture either an unliganded or singly liganded antibody from solution. In this case four binding reactions can be described as follows:

$$A + B_{sur1} \overset{k_{a1}}{\underset{k_{d1}}{\rightleftharpoons}} AB_{sur1},\quad A + B_{sur2} \overset{k_{a3}}{\underset{k_{d3}}{\rightleftharpoons}} AB_{sur2},$$

$$AB_{bulk} + B_{sur1} \overset{k_{a2}}{\underset{k_{d2}}{\rightleftharpoons}} AB_{bulk}B_{sur1},\quad AB_{bulk} + B_{sur2} \overset{k_{a4}}{\underset{k_{d4}}{\rightleftharpoons}} AB_{bulk}B_{sur2}$$

where A represents McAb3D3. AK pre-incubated with McAb3D3 in solution is denoted as B_{bulk}, and the two classes of immobilized AK are denoted by B_{sur1} and B_{sur2}, respectively. AB_{sur1}, AB_{sur2}, $AB_{bulk}B_{sur1}$ and $AB_{bulk}B_{sur2}$ represent the various associated complexes. The differential rate equations were derived according to the reaction mechanisms described above and are presented in Table IV.

It is assumed that the binding of an antigen molecule to an antibody is independent of the status, bound or free, of the antibody molecule. So in the equilibrated AK-McAb3D3 mixture, the following equilibria exist (Eq. 1):

$$A + B_{bulk} \overset{K_{a,s}}{\rightleftharpoons} AB_{bulk},\quad AB_{bulk} + B_{bulk} \overset{K_{a,s}}{\rightleftharpoons} A(B_{bulk})_2,$$
$$K_{a,s} = \frac{[AB_{bulk}]}{[A]\cdot[B_{bulk}]} = \frac{[A(B_{bulk})_2]}{[AB_{bulk}]\cdot[B_{bulk}]}. \quad (1)$$

where $K_{a,s}$ represents the affinity constant in solution. If f is defined as the fraction of bound sites, f can be interpreted as the probability that a randomly selected binding site is bound. So a doubly liganded antibody occurs at frequency f^2. Accordingly, in the equilibrated mixture, the equilibrated concentrations of various components are:

$$[A(B_{bulk})_2] = f^2\cdot A_{tot},$$
$$[AB_{bulk}] = 2\cdot f\cdot(1-f)\cdot A_{tot},$$
$$[A] = (1-f)^2\cdot A_{tot},$$
$$[B] = B_{tot} - 2\cdot f\cdot A_{tot},$$

The total antibody and antigen concentrations are denoted by A_{tot} and B_{tot}, respectively. Substituting the equations above into Eq. 1, we obtain:

$$4\cdot K_{a,s}\cdot A_{tot}\cdot f^2 - (4\cdot K_{a,s}\cdot A_{tot} + 2\cdot K_{a,s}\cdot B_{tot} + 1)\cdot f + 2\cdot K_{a,s}\cdot B_{tot} = 0 \quad (2)$$

With Eq. 2, the relationship between $K_{a,s}$ and f is given by:

$$f = \Big(4\cdot K_{a,s}\cdot A_{tot} + 2\cdot K_{a,s}\cdot B_{tot} + 1 - \sqrt{(4\cdot K_{a,s}\cdot A_{tot} + 2\cdot K_{a,s}\cdot B_{tot} + 1)^2 - 32\cdot K_{a,s}^2\cdot A_{tot}}\Big)\Big/ 8\cdot K_{a,s}\cdot A_{tot} \quad (3)$$

Hence the relationships between the concentrations of various components in the equilibrated mixture and $K_{a,s}$ can be obtained. Thus, $K_{a,s}$ values can be directly fitted using numerical integration algorithms for the differential equations in Table IV.

To determine the affinity constant for binding of AK to McAb3D3 in solution, six different concentrations of AK, between 2.63×10^{-5} and 1.05×10^{-4} M, were mixed with the

TABLE IV. **Differential rate equations of competition reaction models.**

$d[B_{sur1}]/dt = -(k_{a1}\cdot[A]\cdot MW_1\cdot[B_{sur1}] - k_{d1}\cdot[AB_{sur1}])/MW_1 - (k_{a2}\cdot[AB_{bulk}]\cdot MW_2\cdot[B_{sur1}] - k_{d2}\cdot[AB_{bulk}B_{sur1}])/MW_2$

$d[B_{sur2}]/dt = -(k_{a3}\cdot[A]\cdot MW_1\cdot[B_{sur2}] - k_{d3}\cdot[AB_{sur2}])/MW_1 - (k_{a4}\cdot[AB_{bulk}]\cdot MW_2\cdot[B_{sur2}] - k_{d4}\cdot[AB_{bulk}B_{sur2}])/MW_2$

$d[AB_{sur1}]/dt = (k_{a1}\cdot[A]\cdot MW_1\cdot[B_{sur1}] - k_{d1}\cdot[AB_{sur1}])$

$d[AB_{sur2}]/dt = (k_{a3}\cdot[A]\cdot MW_1\cdot[B_{sur2}] - k_{d3}\cdot[AB_{sur2}])$

$d[AB_{bulk}B_{sur1}]/dt = (k_{a2}\cdot[AB_{bulk}]\cdot MW_2\cdot[B_{sur1}] - k_{d2}\cdot[AB_{bulk}B_{sur1}])$

$d[AB_{bulk}B_{sur2}]/dt = (k_{a4}\cdot[AB_{bulk}]\cdot MW_2\cdot[B_{sur2}] - k_{d4}\cdot[AB_{bulk}B_{sur2}])$

$R = [AB_{sur1}] + [AB_{sur2}] + [AB_{bulk}B_{sur1}] + [AB_{bulk}B_{sur2}] + RI$

In these equations, A represents McAb3D3 as the analyte and B_{bulk} represents AK pre-incubated with McAb3D3 in solution; the two classes of immobilized AK are denoted by B_{sur1} and B_{sur2} respectively; R represents the instrument response and RI represents the response from the bulk refractive index effect. MW_1 represents the molecular weight of the analyte (McAb3D3), which is 151.2 kDa. MW_2 represents the molecular weight of singly liganded complexes (AK-McAb3D3), which is 172.6 kDa. The concentrations of various complexes formed during the reaction are expressed in response terms. Thus, differential rate equations directly describe the binding curves obtained with the BIAcore sensor.

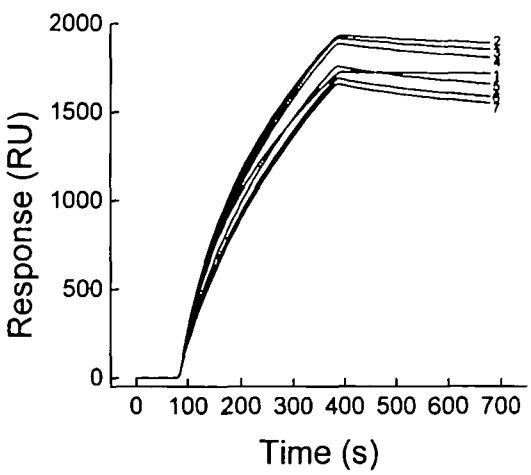

Fig. 3. **Time courses of the association and dissociation for the AK-McAb3D3 equilibrated mixture binding to immobilized AK.** The surface density of AK was the same as in Fig. 1. In the equilibrated mixture, the McAb3D3 concentration was 8.86×10^{-6} M. For curves 1 to 7, the AK concentrations were 0, 2.63×10^{-5}, 3.94×10^{-5}, 5.26×10^{-5}, 7.89×10^{-5}, 9.20×10^{-5}, and 1.05×10^{-4} M, respectively.

TABLE V. **The rate constants and equilibrium constant of AK binding to free McAb3D3 equilibrated with the AK-McAb3D3 mixture.**

R_{max1} (RU)	k_{a1} (M^{-1} s^{-1})	k_{d1} (s^{-1})	K_{a1} (M^{-1})	k_{a2} (M^{-1} s^{-1})	k_{d2} (s^{-1})	K_{a2} (M^{-1})	$K_{a,s}$ (M^{-1})
3.63×10^3	1.53×10^2	1.02×10^{-4}	1.50×10^6	2.23×10^2	2.61×10^{-4}	0.85×10^6	1.10×10^4
R_{max2} (RU)	k_{a3} (M^{-1} s^{-1})	k_{d3} (s^{-1})	K_{a3} (M^{-1})	k_{a4} (M^{-1} s^{-1})	k_{d4} (s^{-1})	K_{a4} (M^{-1})	χ^2
550	2.94×10^3	1.00×10^{-9}	2.94×10^{12}	2.09×10^3	1.00×10^{-9}	2.09×10^{12}	75.9

Curve fitting was performed according to the models in Table IV. Data were taken from Fig. 3.

antibody at a constant concentration (8.86×10^{-6} M) and allowed to reach equilibrium. The resulting sensorgrams are shown in Fig. 3. Following the increase in the AK concentration in the equilibrated mixture, the response value increases and then decreases. This is due to changes in the concentration of singly liganded McAb3D3. The dissociation of the complexes present on the sensor surface was followed after 380 s by injecting the buffer solution. The resulting sensorgrams were fitted by global fitting to the models mentioned above (Table IV). The fitted parameter values obtained are shown in Table V. The equilibrium constants and kinetic constants of free McAb3D3 as to immobilized AK agree well with those obtained in the above experiment (line 3 of Table II). Moreover, the association constants (K_{a1} and K_{a3}) of unliganded McAb3D3 binding to the two classes of immobilized AK are very similar to the association constants (K_{a2} and K_{a4}) of singly liganded McAb3D3. This therefore confirms that it is a reasonable assumption that the binding of an antigen molecule to an antibody is independent of the status, bound or free, of the antibody molecule.

The affinity constant ($K_{a,s}$) of AK-McAb3D3 in solution is 1.10×10^4 M^{-1}, which is significantly lower than the affinity constant for binding of McAb3D3 to immobilized AK or AK to immobilized McAb3D3 ($K_a = 7.21 \times 10^5$ M^{-1} or 6.82×10^5 M^{-1}). This indicates that the affinities determined by surface measurements do not reflect the true binding affinities in solution.

DISCUSSION

The Second Binding Phase for Binding of McAb3D3 to Immobilized AK May Be the Result of Ligand Site Inhomogeneity and Formation of Bridging Complexes—The sensorgrams of the interactions of AK with immobilized McAb3D3 fit well to a pseudo-first-order reaction model. This indicates that when AK is the analyte, it appears homogeneous. However, under conditions where AK is the surface-coupled ligand, the immobilized AK appears inhomogeneous. This inhomogeneity seems to be extrinsic. There are several possible causes of this inhomogeneity of immobilized AK. One possibility is that the chemical immobilization process results in ligands with different affinities (*15, 16*). The major class of immobilized AK shows the same kinetic properties as free AK (line 3 of Table II and line 1 of Table III), so chemical immobilization has no detectable effect on the binding properties of this class of immobilized AK as to McAb3D3. The minor class of immobilized AK may be influenced by the chemical immobilization process, resulting in entirely different kinetic properties.

Steric hindrance of the dextran-immobilized ligands could be a source of their inhomogeneity. The random nature of attachment through covalent coupling could give rise to an array of positions of the analyte-binding region relative to the point of attachment. The random distribution of ligand molecules along the length of the anchoring polysaccharide chain is likely to give rise to a range of affinities, depending on the depth from the carboxydextran microgel surface, and hence the accessibility of the ligand to the analyte. In this case the extent of deviation from pseudo-first-order kinetics should increase with increasing analyte concentration or surface ligand density (*15*)—as the surface ligand density increases, so the number of ligand molecules attached to sites deep within the gel will increase, giving a corresponding increase in the proportion of low affinity sites. The low-affinity sites will be increasingly occupied as the analyte concentration increases, and so more kinetic phases will be observed. However, in our experiments, only two classes of immobilized AK were observed, irrespective of the analyte concentration or ligand surface density. This suggests that the inhomogeneity of immobilized AK did not result from steric hindrance in these experiments.

Conformational changes due to the chemical coupling process are also a possible source of inhomogeneity of immobilized AK. The chemical coupling process could cause conformational changes in the region of AK that is preferentially recognized by McAb3D3. Our previous studies showed that McAb3D3 recognizes a partially denatured conformation of AK rather than the native form (*11*). Such a conformational change could result in a population of immobilised AK with increased affinity for the antibody. This is consistent with the finding that the low-affinity class of immobilized AK has the same affinity constant as AK free in solution. The changes in the kinetic properties of AK due to chemical immobilization appear not to be due to inaccessibility of the binding site, but may be caused by conformational changes of AK itself.

Another possible source of inhomogeneity is the non-uniform distribution of immobilized AK. As antibody McAb3D3 is bivalent, one McAb3D3 molecule can form a bridging complex by binding to two immobilized AK molecules, provided binding occurs in a high surface density region. If a McAb3D3 molecule forms a bivalent bridge, the dissociation rate will be significantly decreased and so the apparent affinity for the chip surface will be far higher than for monovalent binding. Thus, the proportion of the high-affinity binding class of immobilized AK will increase with increasing surface density. This is consistent with our results. When the antibody is the coupled ligand, the AK in the flow phase is monovalent, so the binding of two AK molecules to one McAb3D3 is indistinguishable from that of two AK molecules to two individual McAb3D3 molecules, and so both AK and McAb3D3 appear homogeneous. Hence, another possible explanation for the minor class of immobilized AK is bridging binding by McAb3D3 molecules. It is of course entirely possible that ligand site inhomogeneity and formation of bridging complexes are both present under our experimental conditions.

The Real Constants of Antigen–Antibody Interactions in Solution Can Be Obtained from Competition BIAcore Measurements—The competition BIAcore method was first described by Nieba *et al.* (*17*). In Nieba's experiments the antigens were small organic molecules or peptides, and the mass of the antigen was too small to be detected by the chip surface. So, in their experiments, the response values resulting from the binding of unliganded and singly liganded antibodies to the chip surface were about the same. Therefore the on-rate is simply proportional to the concentration of all other antibody species except that of the doubly liganded antibodies. However, for macromolecular antigens, the response values produced on the binding of a singly liganded antibody are significantly larger than those produced on the binding of an unliganded antibody. Therefore, the observed on-rate is no longer simply proportional to the free antibody combining sites. Thus the ap-

proach provided by Neiba *et al.* could not be directly used for the interaction of macromolecular antigens. To overcome this problem, we modified the method so that the binding constants of a macromolecular antigen as to a bivalent antibody in solution could be evaluated by means of numerical integration algorithms. Also, comparative data, between solution binding and surface binding of AK to McAb3D3, were obtained by the BIAcore method.

In our previous work, the affinity constant of the monoclonal antibody against AK (McAb3D3) was measured by means of an enzyme-linked immunosorbent assay (*11*). When the interaction of the antibody with the immobilized antigen was measured by the direct solid phase ELISA method (*18*), the affinity constant (K_a) of AK binding to McAb3D3 was 8.4×10^8 M^{-1}. When the affinity constant in solution was estimated by partitioning of the antibody between the solid and liquid phase antigen (*19*), a smaller affinity constant (7.0×10^4 M^{-1}) was obtained. It is clear that the affinity constant of $K_{a,s} = 7.0 \times 10^5$ M^{-1} obtained with the solid-phase BIAcore is different from the affinity constants determined by ELISA, while the affinity constants ($K_{a,s} = 1.1 \times 10^4$ M^{-1}) obtained with the competition BIAcore are similar to the one obtained by the partition method. The difference between surface affinities and solution affinities could be due to conformational changes of immobilized ligands. The other possibility is the effect of rebinding (*17*). Rebinding results in smaller apparent dissociation rate constants but has no effect on the binding rate constants.

Global Analysis and Direct Curve Fitting with Numerical Integration as an Improved Method for Analysis of BIAcore Data—Macromolecular interactions observed using surface plasmon resonance technology often exhibit kinetic behavior which deviates from pseudo-first-order kinetics. To deal with this problem, a variety of interpretations and analysis methods have been described in the literature. Some researchers have proposed that deviation from ideal binding progress curves may be a characteristic of the biosensor itself (*20, 21*). Our results show that the binding of a monoclonal antibody to immobolized AK is multiphasic in association and dissociation, and the deviations from pseudo-first-order kinetics are due to inhomogeneity of the immobilized ligands. A similar situation has been observed by others (*15, 22, 23*). Inhomogeneity of the analyte can also produce mutilphasic kinetics, as can a time-dependent step that occurs before or after the initial encounter, for example, a conformational change (*15*). A further cause of deviation from an ideal binding progress curve is the limitation of mass transport from the bulk solution to the sensor (*13*). Therefore, to analyze BIAcore data accurately, it is important to determine the true origin of such deviations. Based on our present work, we suggest that the optimum approach is global analysis and direct curve fitting with numerical integration algorithms, and comparison of the quality of the fit obtained for the various possible models.

REFERENCES

1. Kuby, S.A., Palmieri, R.H., Fischat, A., Fischer, A.H., Wu, L.H., Maland, L., and Manship, M. (1984) Studies on adenosine triphosphate transphosphorylases–amino acid sequence of rabbit muscle ATP-AMP transphosphorylase. *Biochemistry* **23**, 2393–2399
2. Sheng, X.R., Zhang, H.J., Pan, X.M, Li, X.F., and Zhou, J.M. (1997) Domain movement in rabbit muscle adenylate kinase might involve proline isomerization. *FEBS Lett.* **413**, 429–432
3. Zhang, H.J., Sheng, X.R., Pan, X.M., and Zhou, J.M. (1997) Activation of adenylate kinase in denaturants is due to the increasing conformational flexibility at its active sites. *Biochem. Biophys. Res. Commun.* **238**, 382–386
4. Zhang, H.J., Sheng, X.R., Niu, W.D., Pan, X.M., and Zhou, J.M. (1998) Evidence for at least two native forms of rabbit muscle adenylate kinase in equilibrium in aqueous solution. *J. Biol. Chem.* **273**, 7448–7456
5. Zhang, H.J., Sheng, X.R., Pan, X.M., and Zhou, J.M. (1998) Refolding of urea-denatured adenylate kinase. *Biochem. J.* **333**, 401–405
6. Zhang, H.J., Pan, X.M., Zhou, J.M., and Kihara, H. (1998) Activation and conformational changes of adenylate kinase in urea solution. *Sci. China-C* **41**, 245–250
7. Zhang, Y.L., Zhou, J.M., and Tsou, C.L. (1993) Inactivation precedes conformation change during thermal denaturation of adenylate kinase. *Biochim. Biophys. Acta* **1164**, 61–67
8. Zhang, Y.L., Zhou, J.M., and Tsou, C.L. (1996) Sequential unfolding of adenylate kinase during denaturation by guanidine hydrochloride. *Biochim. Biophys. Acta* **1295**, 239–244
9. Zhang, Y.L., Pan, X.M., and Zhou, J.M. (1998) Surface hydrophobicity and thermal aggregation of adenylate kinase. *Biochem. Mol. Biol. Int.* **44**, 949–960
10. Wang, X.D., Luo, J., Guo, Z.Q., Zhou, J.M., and Tsou, C.L. (1997) Pertubation of the antigen-binding site and staphylococcal protein A-binding site of IgG before significant changes in global conformation during denaturation: an equilibrium study. *Biochem. J.* **325**, 707–710
11. Wang, X.D., Zhou, J.M., and Guo, Z.Q. (1997) Preparation and characterization of monoclonal antibodies against adenylate kinase. *Sci. China-C* **40**, 561–567
12. Karlsson, R., Roos, H., Fägerstam, L., and Persson, B. (1994) Kinetic and concentration analysis using BIA technology. *Methods Companion Methods Enzymol.* **6**, 99–110
13. Schuck, P. and Minton, A.P. (1996) Analysis of mass transport-limited binding kinetics in evanescent wave biosensors. *Anal. Biochem.* **240**, 262–272
14. Markey F. (1997) Catering for kinetic awareness. *BIA J.* **4**, 5–9
15. Edwards, P.R., Gill, A., Pollard-Knight, D.V., Hoare, M., Buckle, P.E., Lowe, P.A., and Leatherbarrow, R.J. (1995) Kinetics of protein-protein interactions at the surface of an optical biosensor. *Anal. Biochem.* **231**, 210–217
16. O'Shannessy, D.J., Brigham-Burke, M., Soneson, K.K., Hensley, P., and Brooks, I. (1993) Determination of rate and equilibrium binding constants for macromolecular interactions using surface plasmon resonance: use of nonlinear least squares analysis methods. *Anal. Biochem.* **212**, 457–468
17. Nieba, L., Krebber, A., and Plückthun, A. (1996) Competition BIAcore for measuring true affinities: large differences from values determined from binding kinetics. *Anal. Biochem.* **234**, 155–165
18. Beatty, J.D., Beatty, B.G., and Vlahos, W.G. (1987) Measurement of monoclonal antibody affinity by non-competitive enzyme immunoassay. *J. Immunol. Methods* **100**, 173–179
19. Friguet, B., Chaffotte, A.F., Djavadi-Ohaniance, L., and Goldberg, M.E. (1985) Measurements of the true affinity constant in solution of antigen-antibody complexes by enzyme-linked immunosorbent assay. *J. Immunol. Methods* **77**, 305–319
20. Ito, W. and Kurosawa, Y. (1993) Development of an artificial antibody system with multiple valency using an Fv fragment fused to a fragment of Protein A. *J. Biol. Chem.* **268**, 20668–20675
21. Johanson, K., Appelbaum, E., Doyle, M., Hensley, P., Zhao, B., Abdel-Meguid, S.S., Young. P., Cook, R., Carr, S., Matico, R., McDonnell, P., Morton, T., Bennett, D., Sokoloski, T., McNulty, D., Rosenberg, M., and Chaiken, I. (1995) Binding interactions of human interleukin 5 with its receptor α subunit. *J. Biol. Chem.* **270**, 9459–9471
22. Khilko, S.N., Jelonek, M.T., Corr, M., Boyd, L.F., Bothwell,

A.L.M., and Margulies, D.H. (1995) Measuring interactions of MHC class I molecules using surface plasmon resonance. *J. Immunol. Methods* **183**, 77–94
23. O'Shannessy, D.J. and Winzor, D.J. (1996) Interpretation of deviations from pseudo-first-order kinetic behavior in the characterization of ligand binding by biosensor technology. *Anal. Biochem.* **236**, 275–283